JGSOI (2006) 1: 29-41

Journal of Geological Society of Iran

http://www.gsoi.ir

Characterizing a heterogeneous aquifer by derivative analysis of pumping and recovery test data

N. Samani[1], M. Pasandi[1], D. A. Barry[2]

1. Department of Earth Sciences, Shiraz University, Shiraz 71454 Iran
2. Contaminated Land Assessment & Remediation Research Centre, Institute for Infrastructure and Environment, School of Engineering and Electronics, the University of Edinburgh, Edinburgh EH9 3JN United Kingdom

Abstract Evaluation of aquifer yields with the conventional time-drawdown method is based on the assumption of Theisian or infinite radial flow (IRF) of ground water to a well. However, long-term aquifer yields are controlled by heterogeneities and boundary conditions, which lead to departures from the assumptions underlying the IRF. Accurate prediction of long-term aquifer yields therefore requires evaluation of aquifer heterogeneities. This study involves estimation of Shiraz aquifer parameters from aquifer tests in Fars province, Iran. Aquifer-test responses indicate internal heterogeneity at a scale below the resolution attainable with the available well control. Reliable estimates of aquifer parameters are obtained by applying a derivative technique to the analysis of time-drawdown data. Derivative analysis allows us to identify test segments for which the assumption of IRF is valid. Conventional time-drawdown analyses and derivative curves are then integrated with geological information to identify the nature of heterogeneities and assess their impact on long-term aquifer response to pumping. Finally a conceptual model is proposed for the aquifer.

***Keywords**:* Aquifer test; Derivative time-drawdown analyses; Conceptual model

1. Introduction

Hydrologic test analysis based on the time derivative of drawdown (i.e., rate of drawdown change) with respect to the natural logarithm of time has been shown to improve significantly the diagnostic and quantitative analysis of constant-rate pumping tests. The improvement in test analysis is attributed to the sensitivity of the derivative to small variations in the drawdown change that occurs during testing, which would otherwise be less obvious with standard drawdown–versus-time analysis. The sensitivity of the drawdown derivative to drawdown change facilitates its use in identifying the effects of inner boundaries (wellbore storage, well inefficiencies), outer boundaries (inflow, no-flow), and establishment of various regimes of flow including radial flow conditions on the test.

Standard log-log and semi-log analysis methods used in the interpretation of constant-rate discharge tests depend on assumed Theisian well/formation conditions such as a homogeneous, isotropic, non-leaky aquifer of infinite lateral extent, fully penetrating/communicative well possessing infinitesimally small borehole volumes, and radial laminar flow conditions. It is important that when these conditions and assumptions are not met, their significance on constant-rate discharge test response be understood. Derivative analysis as an aid to aquifer-test interpretation was introduced to the ground water literature by Karasaki et al. (1988), Spane (1993) and Spane and Wurstner (1993). Its origins go back about a decade more in the petroleum engineering literature, specifically the paper by Bourdet et al. (1983). One of the first papers to demonstrate use of pressure derivative to support the analysis of constant-rate discharge tests using the line-source solution was presented by Tiab and Kumar (1980). Following publication of this paper, numerous articles were published, primarily in the petroleum industry, concerning the use of pressure derivative analysis for improving understanding of hydraulic test data and for identifying the flow regime that is operative during the test interval (Bourdet et al., 1983a, b, 1989; Beauheim and Pickens, 1986; Ehlig-Economides, 1988; Horn 1990). The use of pressure derivatives was also extended to the analysis of slug test response within confined aquifers (e.g., Karasaki et. al., 1988; Ostrowskiand Kloska, 1989).

Despite its utility, derivative analysis remains both under-used and under-reported in the hydrogeological literature. The under-use may be due to a lack of published case studies demonstrating the strengths and weaknesses of derivative techniques as applied to conventional aquifer-test analysis.

The purpose of this paper is to highlight the strength of drawdown-derivative analysis in ground water evaluation of a heterogeneous aquifer that exhibits various familiar, yet problematic, hydraulic behavior during aquifer tests. We show that the drawdown–derivative analysis improves estimation of aquifer hydraulic properties and identification of different forms of heterogeneity. Weaknesses of the technique are also shown.

2. Time Derivative of Drawdown Data

During an aquifer test, the hydraulic head in the aquifer declines as the time of pumping increases. Analysis of hydraulic head decline, or drawdown, allows for the estimation of aquifer hydraulic properties. However, the classical Theis solution approach involving log-log type curves of time-drawdown data suffers from problems of non-uniqueness. Semi-log plots based on the Cooper-Jacob (1949) solution are better in this respect, but it can be hard to identify which part of a multi-segmented semi-log time-drawdown curve satisfies the inherent assumption of Theisian or infinite acting radial flow (IRF) to the well.

The drawdown derivative is not taken not with respect to time, t, but with respect to the natural logarithm of time, ln *t*. One of the main problems inherent with the drawdown-derivative approach to transient test analysis is that the rate of change of drawdown, the quantity under consideration, currently cannot be measured directly and must be extracted from discrete measurements of the absolute drawdown evaluation.

The derivative is averaged over a specified abscissa distance before and after the point of interest. The slope of the drawdown derivative for the point of interest is calculated using the following relationship as presented by Mc Connell (1992):

$$t\frac{ds}{dt}\bigg|_i = \frac{ds}{d(\ln t)}\bigg|_i = t_i\left\{\left(\frac{\ln(t_{i+j}/t_i)}{\ln(t_{i+j}/t_{i-k})}\right)\left(\frac{s_i - s_{i-k}}{t_{i-k} - t_i}\right) + \left[\frac{\ln(t_i/t_{i-k})}{\ln(t_{i+j}/t_{i-k})}\right]\left(\frac{s_{i-j} - s_i}{t_i - t_{i+j}}\right)\right\}, \quad (1)$$

Where t_i, t_{i+j} and $t_{i\text{-}k}$ are, respectively, times at the center of the slope, times 0.1-0.5 log cycle later than t_i, and times at least 0.1-0.5 log cycles earlier than t_i; S_i, S_{i+j} and $S_{i\text{-}k}$ are, respectively, the drawdowns at t_i, t_{i+j} and $t_{i\text{-}k}$. Fig. 1 shows representations of ideal drawdown derivative curves for various flow regimes and boundary conditions.

In this paper, for recovery phases following termination of constant-rate discharge tests,

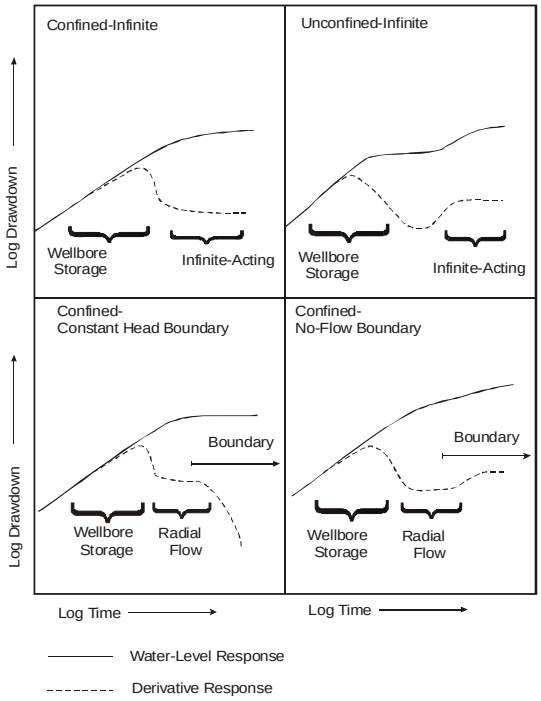

Figure 1. Characteristic log-log pressure and pressure derivative plots for various hydrogeologic formation/boundary conditions (after Spane and Wurstner, 1993).

recovery and drawdown times are converted to a so-called equivalent time function, Δt_e, and recovered drawdown, b, before taking the derivatives. These parameters are defined by Agarwal (1980) and Samani and Pasandi (2001) as, respectively:

$$\Delta t_e = t_P \Delta t / (t_P + \Delta t) \quad (2)$$

and

$$b_t = s_t - r_t \quad (3)$$

where t_p= duration of pumping test [T], Δt= time since pumping terminated [T], and r_t is residual drawdown at time t.

Using the equivalent time function in the differentiation of recovered drawdown data accounts for the length of drawdown time period and allows recovery plots to be analyzed with drawdown type curves (Samani and Pasandi 2003).

3. Geology and hydrogeology of Shiraz plain

Shiraz plain has an approximate surface area of 300 km2. It is located in the central part of Fars province, Iran. The plain falls in zone three (simple folded belt) of the Zagros Orogenic belt and is surrounded by three anticlines, namely, Sabzpoushan in the west, Kaftarak in the east and north and Ghara in the south (Fig. 2). The overall trend of anticlines follows the general NW-SE trend

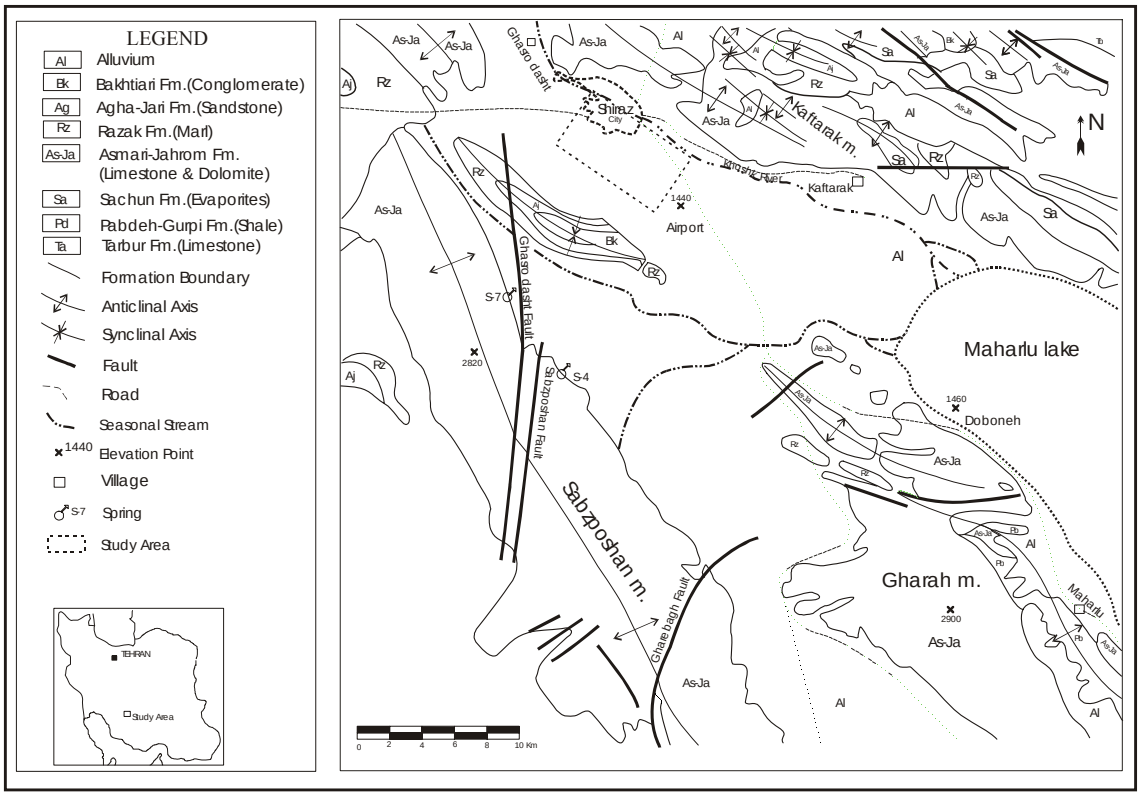

Figure 2. Geological map of the study area (after Samani 2000).

of the Zagros Orogeny. The exposed geologic formations in descending order of age consist of Pabdeh-Gurpi shales and gypsiferous marls (Santonian-Oligocene), Sachun gypsum (Paleocene-L. Eocene), Asmari-Jahrom limestone and dolomite (Paleocene-Oligocene), Razak evaporites (Oligocene-Miocene), Aghajari sandstone (Miocene-Pliocene) and Bakhtiari conglomerate (Pliocene), as shown in Fig. 2. James and Wynd (1965) give more detail on these formations.

The Asmari-Jahrom limestone formation, consisting of joints, fractures and extended voids, is considered as a viable water reservoir recharging the alluvium in certain parts of the plain. On the other hand, the Sachun, gypsum evaporites, and Razak and Aghajari cemented sandstone formations include restrictive permeability and are not important as water-bearing units. The Bakhtiari formation in this area includes conglomerate with hard cemented limestone matrix and is also a poor water reservoir.

Quaternary alluviums of Shiraz plain vary from coarse grained sediments and alluvium fans in surrounding highlands foot to fine grained lake sediments close to Maharlu lake. To the north and northwest of the plain, sediments are mainly coarse grained and contain gravel, sand and pebbles which are generated from the erosion of surrounding limestone highlands and sedimentation along the Khoshk river. In the central part, sediments are often medium grained and comprise gravel and sand along with a mixture of silt and clay. In addition to surface variations, the size and sorting of sediments vary with depth.

The only exit point of the Shiraz aquifer is located at the southeastern part of the plain, where water discharges to Maharlu Lake (Parab, 1991).

4. Derivative-assisted evaluation of the Shiraz aquifer

Data from three sites in the Shiraz aquifer were analyzed. The data set included information from four pumping wells and five observation wells (piezometers). The analysis was conducted on data from both pumping and recovery stages and includes the Theis type curve matching method and the Cooper-Jacob semi-log approximation and derivative techniques. The following sections describe integrated interpretation of drawdown data by these methods in these sites.

Site 1: Deh-Pialeh

In this site a constant-rate pumping test of 763.2 m^3/day was performed in a well 50 m deep. Drawdown was measured in the pumping well and in a piezometer 18 m deep located 6.1 m from the

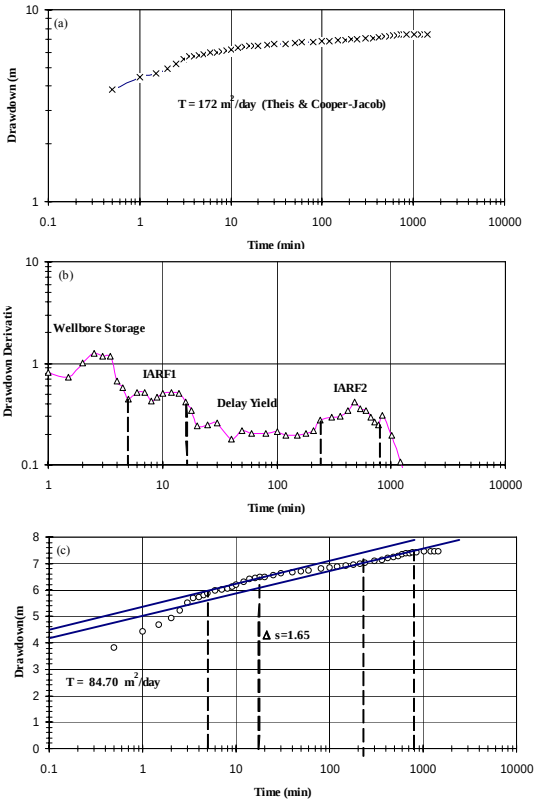

Figure 3. Deh-Pialeh pumping well (50 m deep) drawdown data.

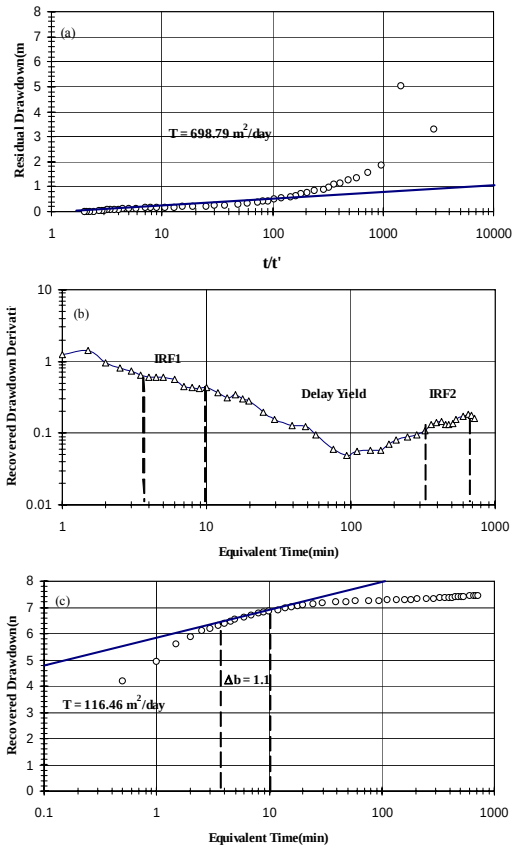

Figure 4. Deh-Pialeh pumping well (50 m deep) recovery data.

pumping well. After 1000 minutes of pumping, the pump was stopped and the recovery drawdown recorded in both wells for 800 min. Fig. 3 represents pumping test results of the pumping well. The derivative curve (Fig. 3b) consists of a hump (the first 5 minutes) two linear segments with zero slopes (5-15 min and 250-800 min) and a depression (15-250 min). The hump, the depression and the linear segments are indicative of wellbore storage, delayed yield and IRF, respectively.

The presence of two IRF segments and delayed yield between them in the derivative curve reflects typical unconfined aquifer behavior at Deh-Pialeh site.

The conventional log-log representation of pumping data (Fig 3.a), in contrast to the derivative curve (Fig. 3.b), lacks a diagnostic shape. Although, the semi-log plot (Fig. 3.c) consists of four distinctive segments, differentiation of the segments satisfying the IRF regime is rather subjective. But, with the help of the derivative curve various components of flow including wellbore-storage, delay-yield and the IRF are more easily distinguished. The IRF segments are used to calculate transmissivity and storage coefficient of the aquifer.

Recovery results of this well also show this characteristic. Fig. 4a is the standard residual drawdown plot of the pumping well as suggested, e.g., by Todd (1986) and Fetter (2001). For a homogeneous aquifer, this plot should appear as a straight line, in which case the second segment of Fig. 4a is indicative of heterogeneous behavior of the Deh-Pialeh aquifer. The early IRF is difficult to distinguish from delayed yield and the value of transmissivity is unrealistically large (T = 698.78 m^2/day). Note that from this kind of plot estimation of the storage coefficient is not possible (Todd 1986, p. 133). The residual drawdown was converted to recovered drawdown (according to Samani and Pasandi 2001) and the derivative curve of recovered drawdown data plotted in Fig. 4b. The two IRF and delayed yield components are distinguishable. Having separated the IRF data, the semi-log plot of Fig. 5c provided transmissivity values comparable to the value in Fig. 3c.

Fig. 5 represents the pumping test response data taken from the piezometer at Deh-Pialeh site. The three presentations in Fig. 5 reflect the heterogeneity of the aquifer. While the log-log plot (Fig. 5a) may be matched with Theis type curve, the derivative curve and the semi-log plot provide a better diagnostic tool for differentiating the IRF regime. Although the second IRF segment is not

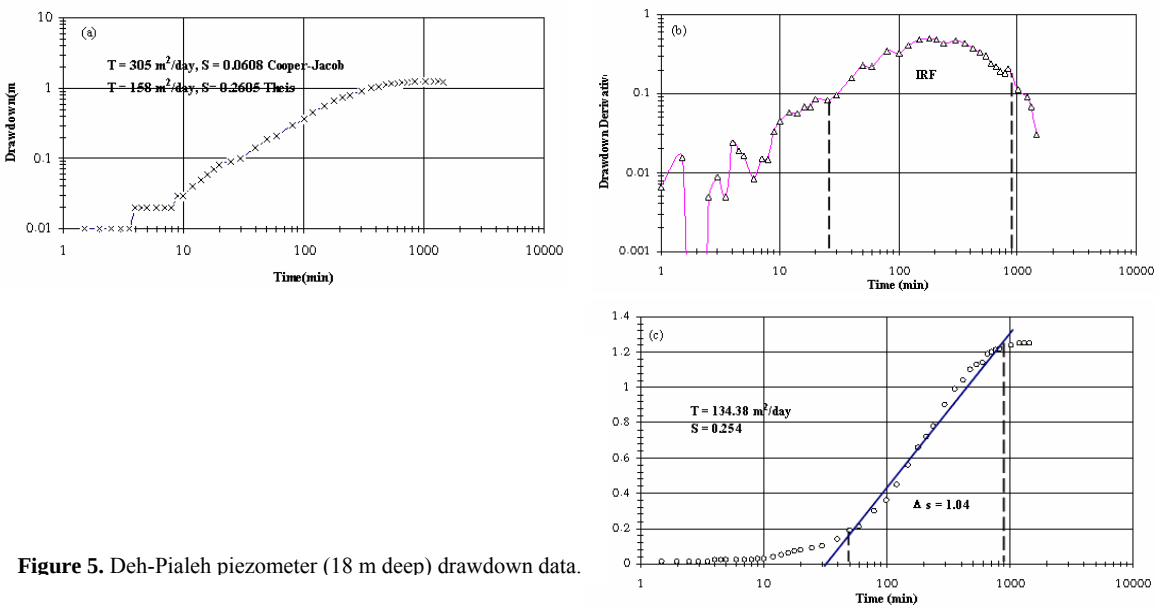

Figure 5. Deh-Pialeh piezometer (18 m deep) drawdown data.

observed in Fig. 5, the high storativity value calculated from the pumping test response data in this piezometer is more representative of an unconfined aquifer (i.e., storativity of 0.254). Fig. 6 represents the recovery data at the piezometer. While the derivative curve separates the two IRF components, the semi-log plots hardly show any delayed yield, particularly in the absence of the

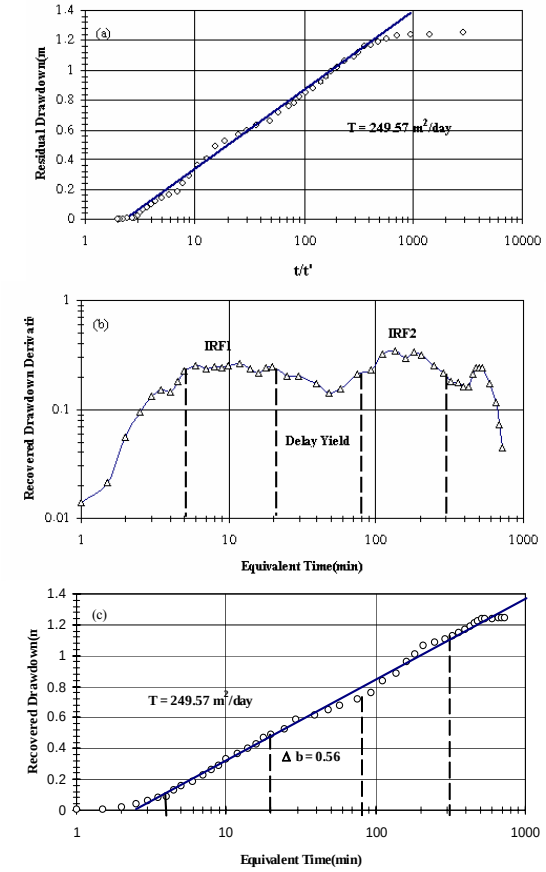

Figure 6. Deh-Pialeh piezometer (18 m deep) recovery data resulting from switching off the 50 m deep pumping well.

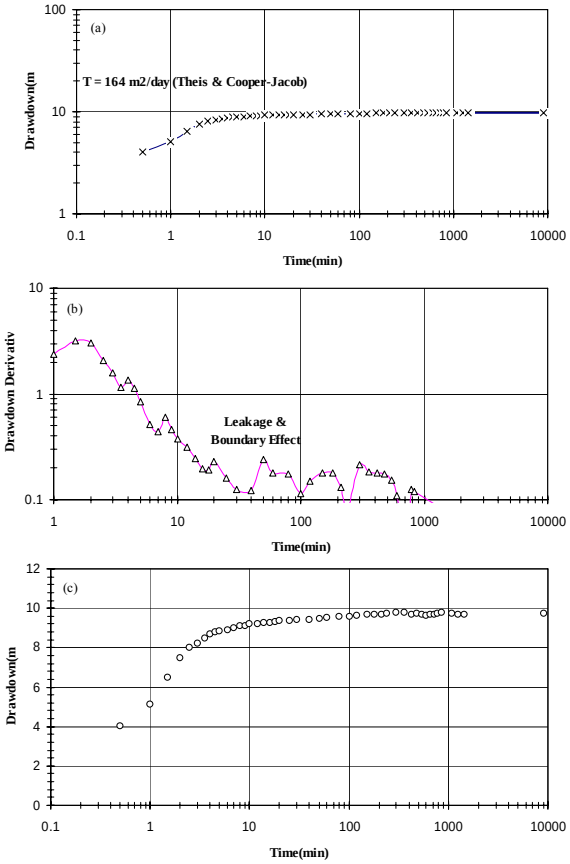

Figure 7. Dashte-Chenar pumping well (50 m deep) drawdown data.

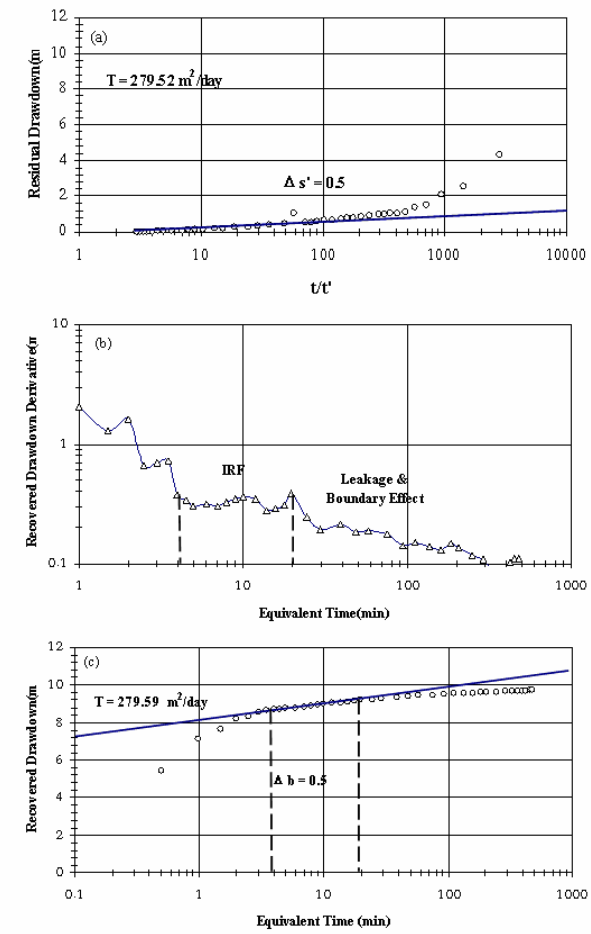

Figure 8. Dashte-Chenar pumping well (50m deep) recovery data.

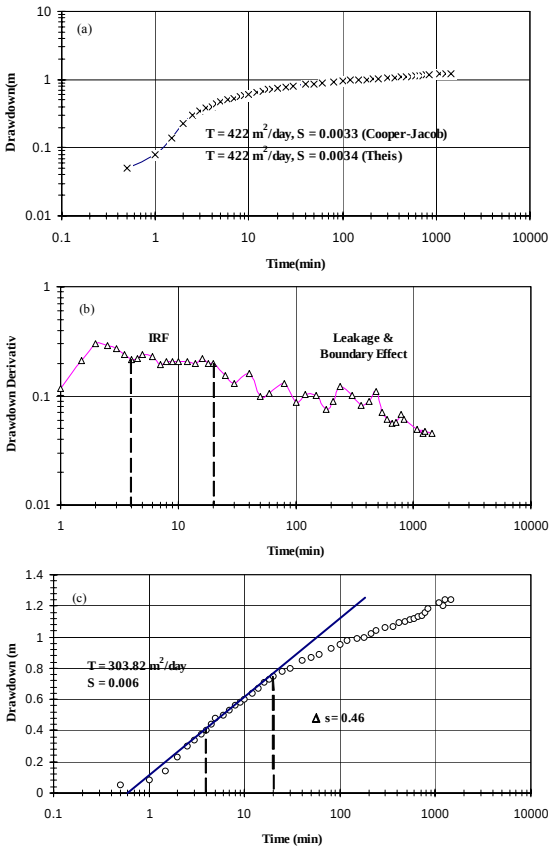

Figure 9. Dashte-Chenar piezometer (18m deep) drawdown data**.**

derivative curve. Conventional graphical representations of recovered data (Figs. 6a and 6c) lack any diagnostic shape and the whole data almost appear as IRF, as a result transmissivity is somewhat overestimated compared to Fig. 3.

Site 2: Dashte-Chenar

At this site two pumping tests were performed in two wells 50 and 300 m depth.

a) Shallow aquifer

Water was pumped from a well 50 m deep at a constant discharge rate of 763.2 m^3/day. Drawdown was simultaneously measured in the pumping well and in a 18 m deep piezometer, 6.6 m away. Data from the pumping well are exhibited in Fig. 7. The derivative curve (Fig. 7b) indicates that nearly all pumping test data are affected by a source of recharge. This is due to combined effects of leakage through confining layers and recharge from a drainage canal 4 m deep, located 70 m north of the well. The derivative curve also indicates that any estimates of S and T from the data in Fig. 7a would be in error in the absence of the IRF. The semi-log plot (Fig. 7c) is not informative either.

In Fig. 8 the recovery test data from the pumping well are plotted. A radial flow segment can be distinguished at the beginning (4-20 min) through the derivative curve and my be utilized for transmissivity determination in the semi-log plot of Fig. 8c (T = 279.52 m^2/day). But, with a more careful review, it is deduced that the separated segment is a pseudo-radial flow and my not be valid for transmissivity determination. This is because the recovery data are also affected by the leakage from the drainage canal from the beginning of the recovery stage. Therefore, the leakage inherent in the pumping phase results affect recovery results from the starting time. This matter can be distinguished from the decline of the curve at the primary stages of the recovery.

The derivative curve of the piezometer (Fig. 9b) not only shows an IRF segment but also illustrates the effect of a recharge boundary and suggests that the Theis curve matching and semi-log estimations of S and T must be carried out on a selected portion

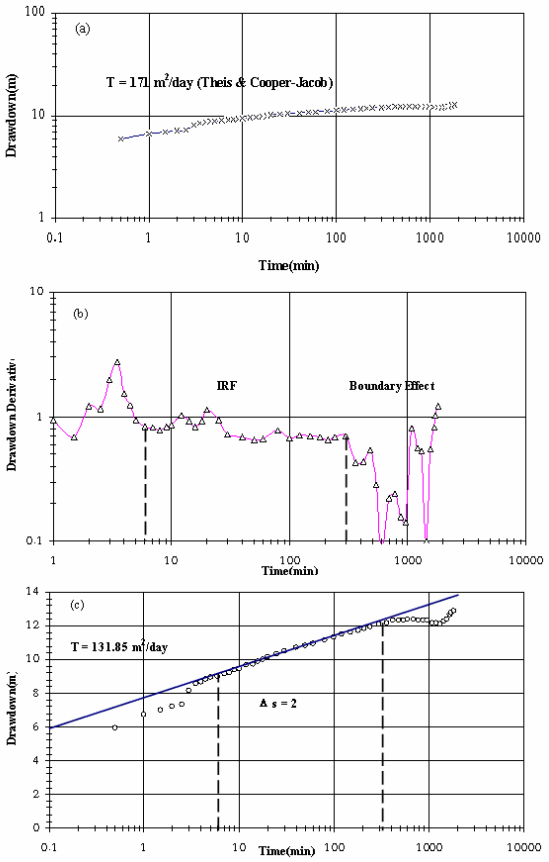

Figure 10. Dashte-Chenar Pumping well (300m deep) drawdown data.

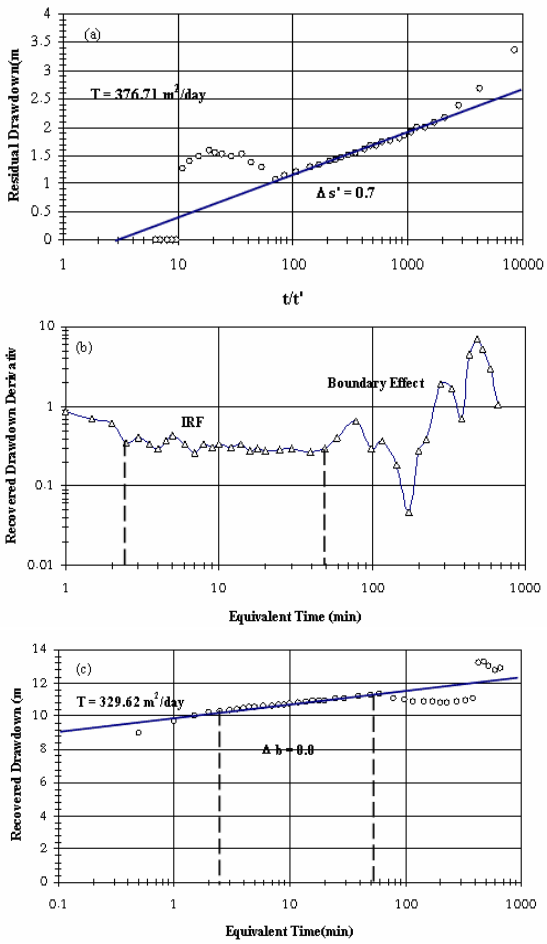

Figure 11. Dashte-Chenar Pumping well (300m deep) recovery data.

of data i.e., data from 4 to 20 min of pumping (see Figs. 9a and 9b).

b) Deep Aquifer

A pumping test was performed on a 300 m deep well at a constant discharge rate of 1440 m3/day. Drawdown during the pumping period was measured in the pumping well and in a 132 m deep piezometer and in the 18 m deep piezometer. The first piezometer is located 15 m and the second 11 m away from the pumping well. After pumping for 4000 min the water level rise was recorded for a period of 700 min. Fig. 10 illustrates the time-drawdown relation for the pumping period in the pumping well. Fig. 10a is the log-log plot, Fig. 10b is the drawdown derivative curve and Fig. 10c is semi-log plot. The derivative and semi-log plots indicate the presence of the IRF and the recharge boundary. Again, the value of T is estimated from the IRF segment using semi-log plot, with the result T = 329.62 m^2/day. The recharge boundary is the water canal 85 m away from the pumping well which affects the drawdown after 300 minutes of pumping.

Fig. 11 depicts the respective recovery plots with similar components of flow as Fig. 10. However, it is interesting to notice that the recharge boundary affects the recovery only after 60 min. From this it is inferred that a considerable percentage of the drawdown is recovered (well loss component) at the early minutes of recovery, a situation that reflects the inefficiency of the pumping well.

Fig. 12 shows the time-drawdown relation for the 132 m deep piezometer with a lower rate of drawdown. The IRF starts a few minutes after pumping and extends to the 300 min before the water canal recharges the cone of depression. The log-log plot (Fig. 12a) shows a more homogeneous behavior compared with Fig. 7a (for a shallow aquifer). It also resembles behavior of a confined aquifer or that of an unconfined aquifer with a large saturated thickness.

Fig. 13 illustrates recovery data of the 132 m deep piezometer. In Figs. 14 and 15 pumping test and recovery test results of the piezometer at 18 m depth are plotted. From the rate-of-drawdown derivative and the recovered drawdown derivative,

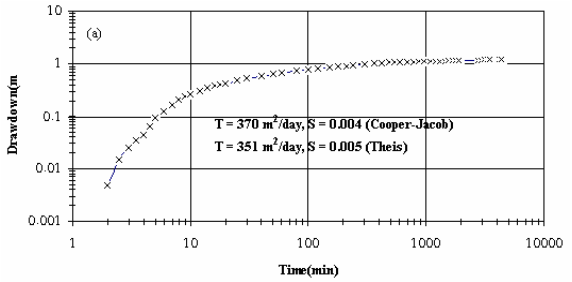

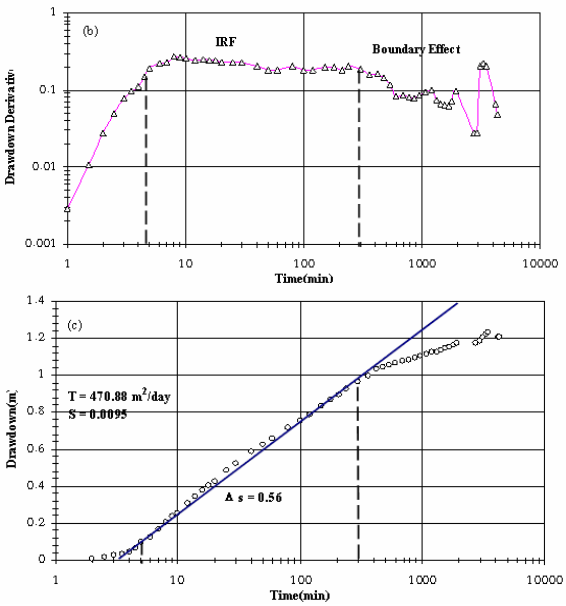

Figure 12. Dashte-Chenar piezometer (132m deep) drawdown data.

which are lower than those of pumping test on shallow wells, it is deduced that this well is affected by the leakage and boundary effects more than pumping with smaller discharge in shallow wells. That large values of T were calculated from the data in these figures confirms this idea. Regarding the drawdown-time derivative curve for deep wells, the time required for the cone of depression to reach the inflow boundary is proportional to the distance from the drainage canal. The time can be read on the derivative curve. For the 300 m deep pumping well (Fig. 10) it is 300 min while for the 132 m deep well it is 200 min. For the recovery stage, these times reduce to 52 min (Fig. 11) and 38 min (Fig. 13), respectively.

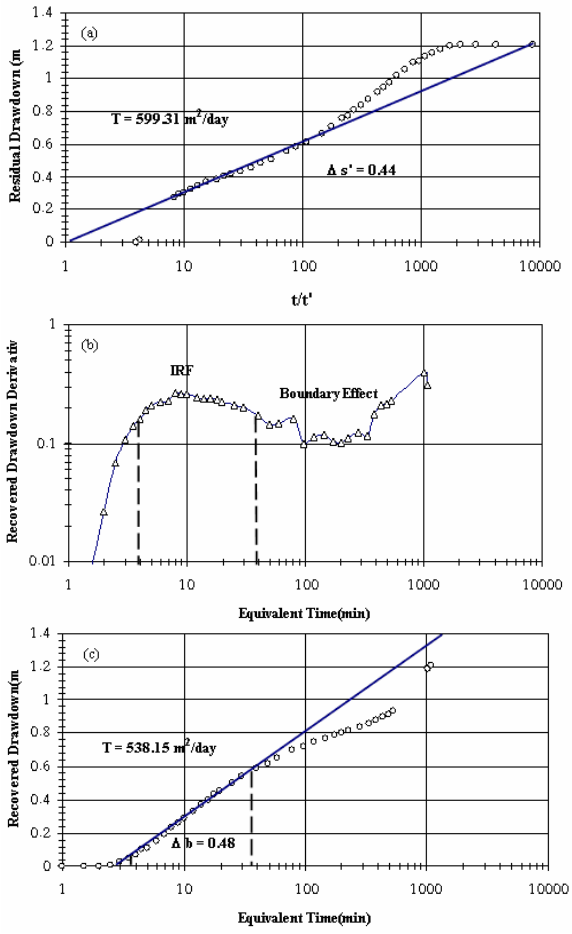

Figure 13. Dashte-Chenar piezometer (132m deep) recovery data.

Site 3: Katasbes vilage

A constant discharge test was conducted on a 42 m deep well in this site. The drawdown data in both pumping and recovery periods were recorded in the pumped well and in a piezometer 18 m deep. The piezometer was situated 4.70 m away from the pumped well. Time-drawdown data for the pumped well is illustrated in Fig. 16. Figure 16a does not show clear Theis type curve characteristics and reflects heterogeneous behavior. The derivative curve (Fig. 16b), however, consists of three segments. First, a hump indicative of wellbore storage and inefficiency, second an IRF segment, and third a probable recharge source. The slope of IRF segment in semi-log plot (Fig. 16c) is 1.6m/log cycle, which gives a value of 84.05 m^2/day for T.

Fig. 17 shows the result of aquifer test in the piezometer. The similarity between the presentations of this figure with their corresponding presentations in Fig. 16 is clear. Due to short distance between the wells, the wellbore effect is also observed in the piezometer data. The T values calculated from the semi-log plots (Fig. 16c and Fig. 17c) are very close to each other, but deviate

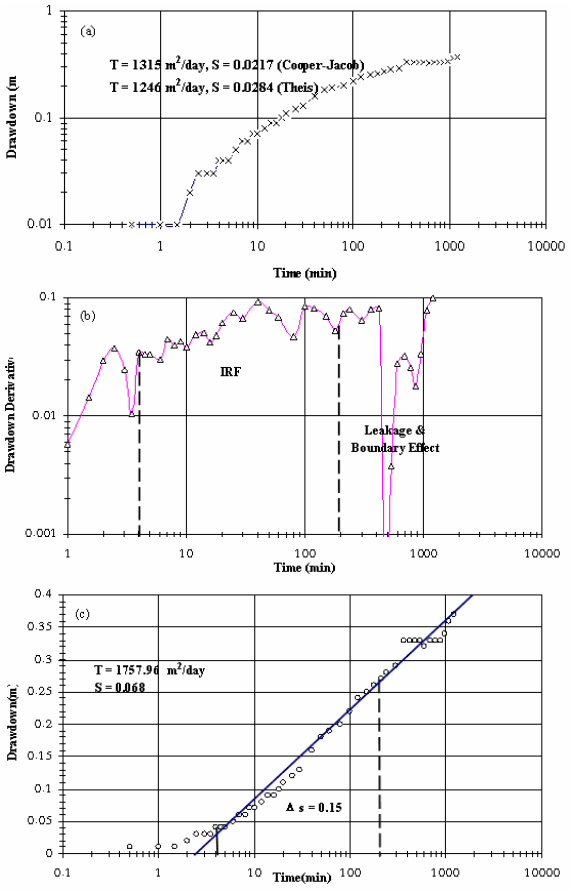

Figure 14. Dashte-Chenar piezometer (18m deep) drawdown data resulting from pumping of 300m deep well.

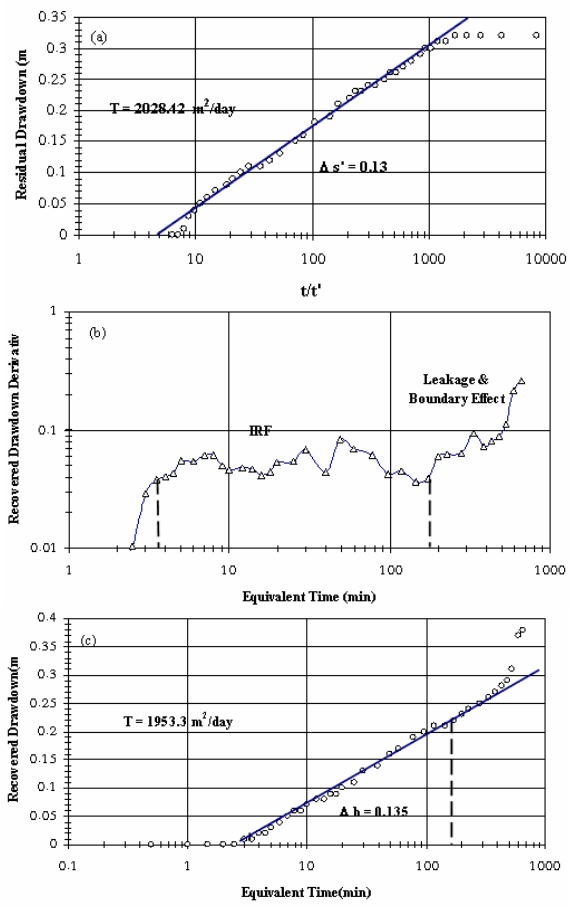

Figure 15. Dashte-Chenar piezoeter (18m deep) recovery data resulting from switching off the 300m deep pumping well.

from values calculated by log-log plots (Fig. 16a and Fig. 17a). The scatter evident in the log-log plots indicates that T values calculated by semi-log plots are more reliable.

Fig. 18 shows recovered drawdown data at the recovery stage in the pumped well. These data show a similar shape to the curves for the pumping data and the calculated values of T are close also. A hump indicative of wellbore storage and inefficiency effects at the beginning of the derivative curve and then a radial flow horizontal line is delineated. If the increased rate of drawdown-change within the drawdown phase is compared with the increased rate of recovery on the corresponding derivative recovery curve, it can be seen that the beginning of the horizontal radial flow segment during recovery (i.e., 0.35 m/log cycle) is a little lower than the horizontal line during drawdown phase (i.e., 0.6 m/log cycle). Therefore, the end segment of the recovered drawdown derivative, which is located at the same level of the radial flow segment during the pumping phase (i.e., 0.6m/log cycle), is considered as a real radial flow segment. This phenomenon, which is also observed in some derivative graphs of other sites, is due to heterogeneity of the aquifer.

Fig. 19 presents data for recovery of the piezometer. In the derivative curve (Fig 19b) and semi-log plot (Fig. 19c), the IRF persists for a longer time but the value of T calculated by this curve is close to that from pumping data.

5. A Conceptual model for Shiraz Aquifer

The Shiraz plain consists of alternating pervious and semi-pervious strata (Samani 2000, Parab, 1991). Different aquifer strata exhibit different hydraulic head and hydraulic conductivity. Since all the wells are fully screened (from few meters below water table to their full depth), the measured head in any well reflects a weighted average of the individual heads in various strata, that is:

$$\phi = \frac{\sum T_i \phi_i}{\sum T_i} \qquad (4)$$

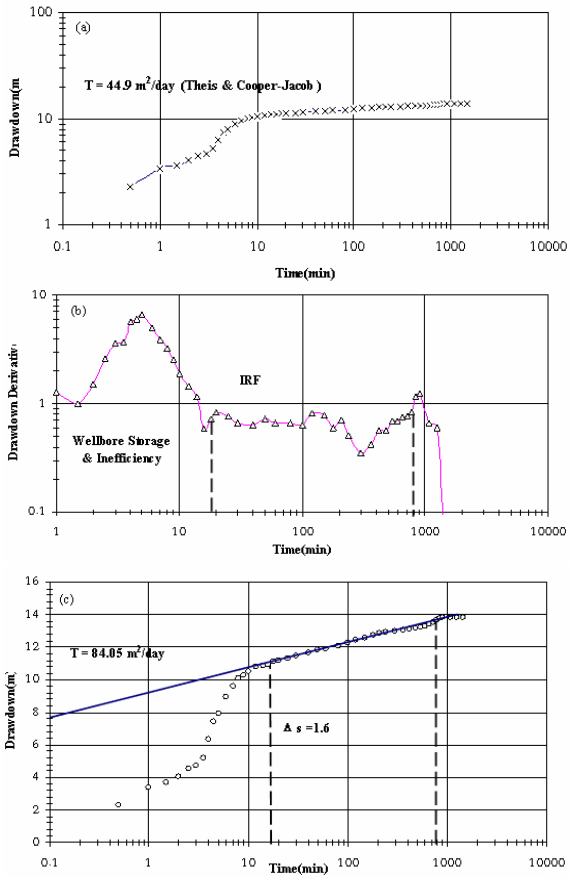

Figure 16. Katasbes pumping well (42m deep) drawdown data.

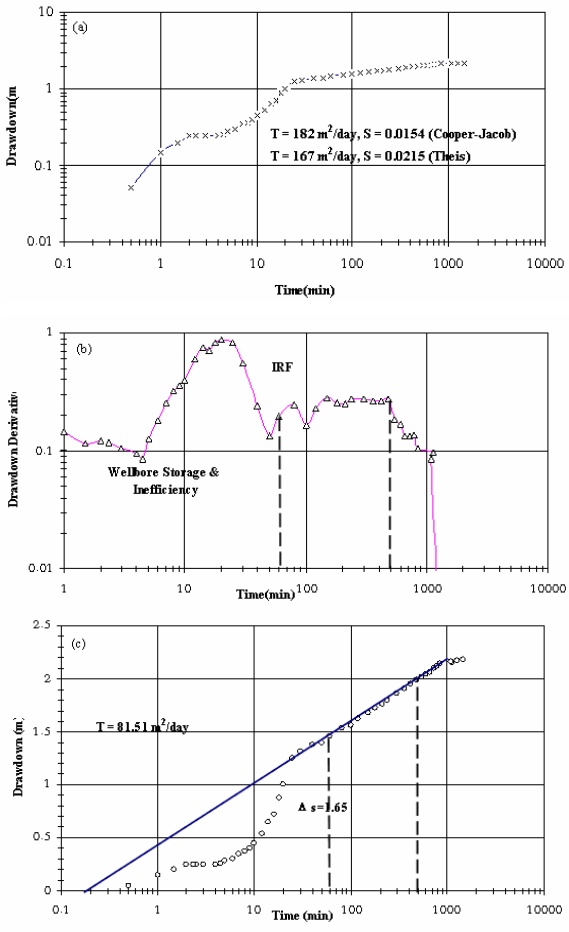

Figure 17. Katasbes piezometer (18m deep) drawdown data.

where T_i and Φ_i are the transmissivity and head of the ith aquifer (Haitjema, 1995).

The Shiraz aquifer may be modeled most simply as two major water-bearing strata separated by an aquitard. Depending on the pumping depth and screen length, the aquitard acts as a leakage path from the superficial unconfined aquifer to the deep confined aquifer or vice versa. Fig. 20 is the suggested conceptual model for Shiraz aquifer. Such a model may respond to stresses in the following ways:

a) In wells, where the flow contribution of the unconfined aquifer is higher than that of the confined aquifer (in other words when the rate of water table decline is larger than that of piezometer level), the leakage through the aquitard is upward. In such cases, in the beginning of pumping period, the flow mechanism in the unconfined aquifer will match the Theisian flow (or IRF). As pumping continues, upward leakage takes place and the rate of drawdown decreases. On the derivative drawdown curve the Theisian flow has a horizontal pattern, after which it follows a descending trend. Such a mechanism is observed in Figs. 9, 14, and 17. Note that these figures belong to wells reaching depths of 18 to 42 m. These are shallow wells fed by the superficial unconfined aquifer.

b) In wells, where the flow contribution of the confined aquifer is higher than that of the unconfined aquifer (i.e., where the rate of the piezometer level decline is higher than that of the water table), the leakage through the aquitard is downward. For such cases, the early response to pumping will match Theisian flow. As pumping continues the downward leakage will slow the rate of drawdown. On the derivative drawdown curves the Theisian flow component takes a horizontal pattern and then, as a result of downward leakage, it follows a descending trend. This mechanism is observed in Figs. 8, 10, 12, 16 and 18. Note that these figures are related to wells with depths of 50m and greater. For even higher leakage rates, the Theisian flow and derivative curves follow a descending trend from the moment pumping starts (Fig. 7). In such cases

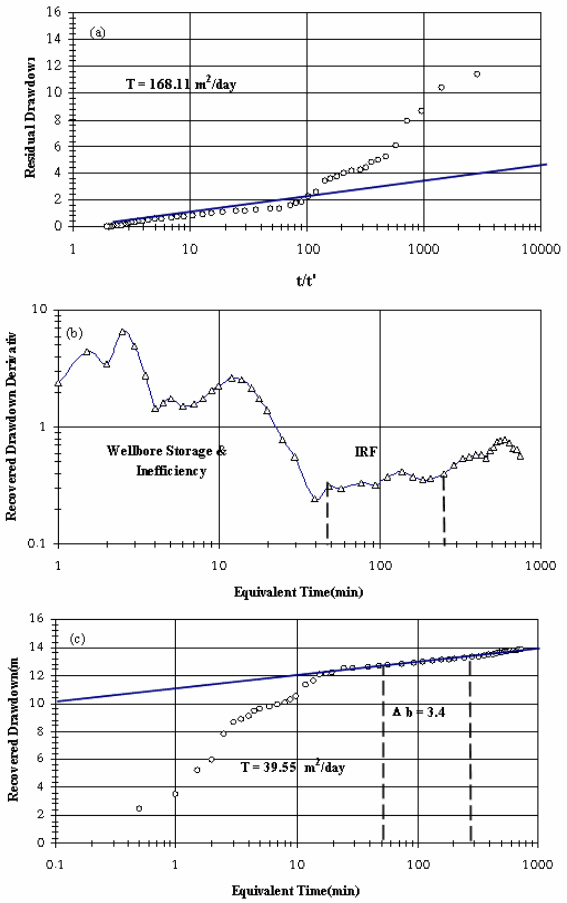

Figure 18. Katasbes pumping well (42m deep) recovery data

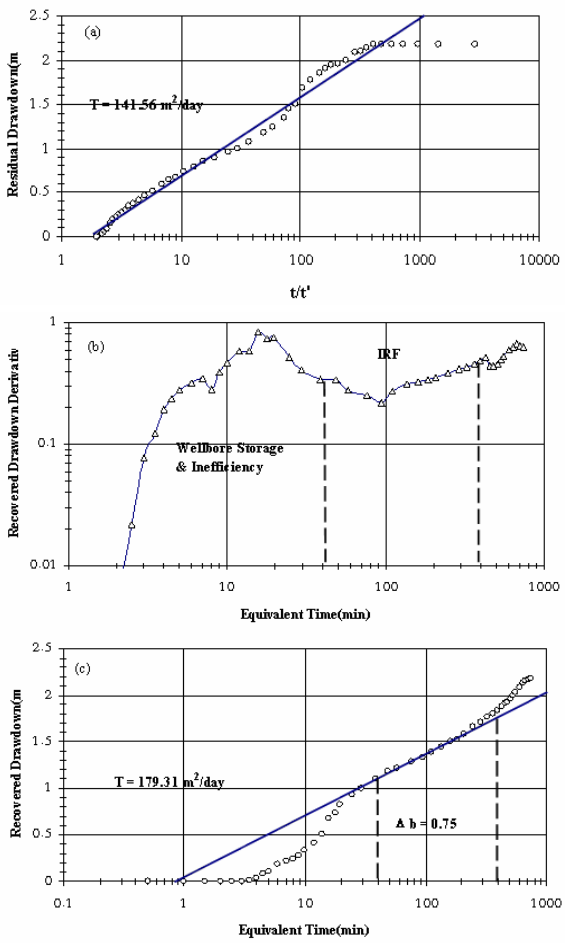

Figure 19. Katasbes piezometer (18m deep) recovery data.

the pumping test data should not be used for calculation of S and T.

In both the above cases, when the pump is switched off the recovery starts and the recovery derivative curve follows a horizontal (Theisian flow) and then an ascending trend (leakage), as shown in Figs. 11, 15, and 19.

c) Where the thickness of aquifer in comparison to that of aquitard is large or the system behaves as an unconfined aquifer; the derivative curve in both the pumping and recovery phases will exhibit three components: early Theisian flow, delayed yield and, finally, late Theisian flow (Figs. 3-6).

6. CONCLUSIONS

The derivative-assisted method originally used in petroleum engineering is a powerful diagnostic tool for analyzing hydrologic well-test data. It has a great advantage of differentiating various regimes and components of flow.

Conventional methods of well-test data analysis, i.e., both computer-aided and manual type curve matching and semi-log straight-line analyses were performed on the whole data set rather than the infinite radial flow data. As a result the values calculated for *T* and *S* are not always representative of the aquifer tested.

The accuracy of data can be also checked by this method of analysis. Differentiation is a noise producing process. So, erroneous data generate a lot of noise and may not be applicable for calculation of aquifer parameters. Long intervals of drawdown measurements also produce noise in the derivative plot. This method can be used to depict real response of wells for selection of a suitable analytical model of analysis (model identification).

Due to inner boundary effects on the pumping well data, conventional methods of aquifer parameter evaluation require construction of a piezometer with a rather high cost. In contrast, the derivative method separates the Theisian flow component, so there is no need for a piezometer and considerable amount of money is saved.

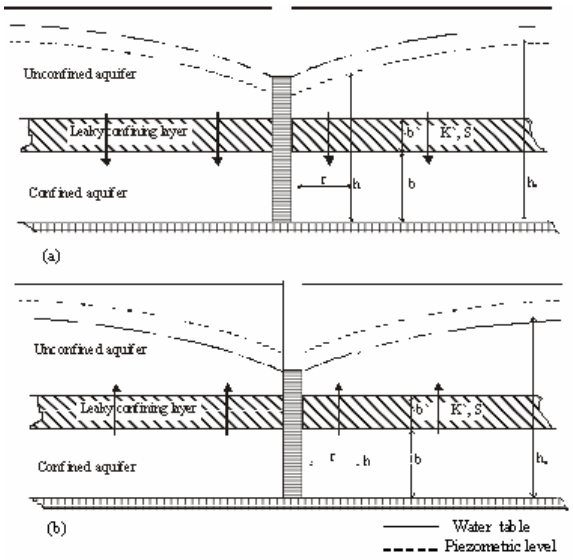

Figure 20. A conceptual model for Shiraz aquifer, a) leakage from upper aquifer to lower one, b) leakage from lower aquifer to upper one.

It is recommended that a data-logger is used for continuous recording of water level with equal intervals during pumping for reduction of noise in the derivative plot.

Pumping test data from several sites in Shiraz plain were analyzed by conventional as well as derivative methods. Derivative plots of well-test data delineated various inner and outer boundary conditions in the aquifer. Different forms of heterogeneity were found among the well tests; these were confirmed by field evidence. Based on the pumping test data and their analysis, a conceptual model was proposed for the aquifer, in which it was proposed to consist of an upper unconfined aquifer, an aquitard, and a lower semi-confined aquifer.

7. Acknowledgement

This paper was completed when the first author was on a sabbatical leave at the University of Edinburgh, UK. Financial support provided by Shiraz University, Iran is acknowledged.

References

Agarwal, R.G. 1980, *A new method to account for producing time effects when drawdown type curves are used to analyze pressure build up and other test data*, Presented at the Society of Petroleum Engineers Annual Technical Conference and Exhibition, Sept.21-24, Dallas. SPE paper 9289.

Beauheim, R. L., & Pickens J. F.1986, *Applicability of pressure derivative to hydraulic test analysis*. Paper presented at poster session at the Annual Meeting of Am. Geophys. Union, Baltimore, MD, May 19-22.

Bourdet, D., T.M. Whittle, A. A. Douglas, and Y.M. Pirard. 1983a, A new set of type curves simplifies well test analysis, *World Oil*, May 1983, pp.95-106.

Bourdet, D., J. A. Ayoub, T.M. Whittle, Y.M. Pirard, and V. Kniazeff. 1983b. "Interpreting well tests in fractured reservoirs." *World Oil*, October, 1983, pp.77-78

Bourdet, D., J. A. Ayoub, Y. M. Pirard. 1989, *Use of pressure derivative in well-test interpretation*. Society of Petroleum Engineers, SPE Formation Evaluation, June 1989, pp. 293-302

Cooper, H. H., Jr., &. Jacob, C. E. 1946, A generalized graphical method for evaluating formation constants and summarizing well-field history. *American Geophysical Unio, Transactions* 27(4): 526-534.

Ehlig-Economides, C., 1988, Use of the pressure derivative for diagnosing pressure-transient behavior, *Journal of Petroleum Technology*, October 1988, pp. 1280-1282.

Fetter, C.W. 1992, *Applied Hydrogeology*. Prentice, Englewood cliffs, NJ07632.

Haitjema, H. M. 1995, *Analytic element modeling of groundwater flow*, Academic Press, 393 pp.

Horn, R. N. 1990, *Modern well test analysis: A computer-aided approach.* Petroway, Inc., Palo Alto, California; Distributed by the Society of Petroleum Engineers. Richfield, Texas.

James, G. A. and Wynd, J. G., Stratigraphic nomenclature of Iranian Oil Consortium Agreement Area: *Bulletin of the American Association of Petroleum Geologists*, v. 49, no. 12, p. 2182-2245.

Karasaki, K., J.C.S. Long and P.A. Witherspoon, 1988, Analytical models of slug tests, *Water Resources Research*, v.24, no.1, p.115-126

McConnell, C. L. 1993, Double porosity well testing in the fractured carbonate rocks of the Ozarks. *Ground Water*, 31(1), 75-83.

Ostrowski, L. P. and M. B. Kloska, 1989, *Use of pressure derivatives in analysis of slug test or DST flow period data*. Soc. Pet. Engrs., SPE paper 18595.

Parab. 1991, *Water table decline in south-eastern of Shiraz plain: 3rd book, Studies of Ground Water Resources,* 259 pp.

Samani, N. 2000, Stochastic Response of Karst Aquifers to Rainfall and Evaporation, Maharlu Basin*, Journal of Cave and Karst Studies* 63(1), April.

Samani, N. and Pasandi, M. 2003, A single recovery type curve from Theis'exact solution, *Ground Water*, Vol. 41,No. 5.

Spane, F.A., Jr. 1993, *Selected hydraulic test analysis techniques for constant-rate discharge tests,* Pacific Northwest Laboratory 8539, Richland, W.A, pp.80

Spane, F. A., Jr. and S. K. Wurstner., 1992, *DERIV: A program for calculating pressure derivatives for*

hydrologic test data. PNL-SA-21569, Pacific Northwest Laboratory, Richland, Washington.

Tiab, D. and A. Kumar, 1980, Application of the *PD*' function to interface analysis*, J. Pet. Tech.* August, pp. 1465-1470.

Todd, D.K. 1986*, Ground Water Hydrology*. John Wiley & Sons, New York.

Walton, W.C. 1970, *Groundwater Resources Evaluation*. McGraw-Hill Series Book Company.